

SCALING FOR ICING WIND TUNNEL TESTS AND VALIDATION WITH NUMERICAL SIMULATIONS

Gizem Ozbek Yanmaz¹
TUBITAK-SAGE
Ankara, Turkey

Prof. Dr. Serkan Ozgen²
Middle East Technical University
Ankara, Turkey

ABSTRACT

Objective of the study is to employ a scaling method that produces scaled ice accretions over a wide range of test conditions and to validate the method before the icing wind tunnel tests. A scaling method for size and test-condition scaling that is based on similitudes of geometry, flow field, droplet trajectory, water catch, energy balance and surface water dynamics is validated with icing analyses for reference and scaled conditions using FENSAP-ICE software and an in-house icing code AEROMSICE-2D. The ice accretions obtained by analyses are compared with experimental data and the scaling method is tested for several Appendix-C icing conditions. Comparisons of reference and scaled results show good agreement.

INTRODUCTION

Icing is one of the most dangerous hazards to be encountered by air vehicles in flight. The formation of ice on aircraft surfaces occurs during flight through supercooled droplets. Supercooling is the state in which water exists as a liquid at a temperature below 0°C. Cloud droplets may freeze instantaneously and form rime ice or run downstream and freeze later forming glaze ice structure. Ice accretion, particularly on control surfaces, wings and flight data sensors usually degrades both performance and operational safety of air vehicles. Thus, it has become important in the design and certification phases of system development to evaluate performance degradation because of icing. Ice accretion prediction may be performed by numerical analyses. Nevertheless, there exists a necessity of icing tests, for validating the numerical analyses and/or for certification purposes. Test methods for evaluating the performance characteristics of aircraft in icing conditions are flight tests in natural icing conditions, simulated clouds produced by icing tankers and ground testing in icing wind tunnels. Icing wind tunnel testing is the most convenient method considering feasibility, cost and safety. However, when full-size model is too large for a given facility or when the desired test conditions are out of the operating capability of the facility, requirement of a scaling method that produces scaled ice accretions for extensive test conditions arises. The scaling method shall be validated before the icing wind tunnel testing for reliability and validity of the tests. This work illustrates a scaling method for size scaling and test-condition scaling that is based on similitudes of geometry, flow field, droplet trajectory, water catch,

¹ MSc. Student in Aerospace Engineering Department and Research Engineer at TUBITAK-SAGE, Email: gizem.ozbek@tubitak.gov.tr

² Prof. Dr. in Aerospace Engineering Department, Email: serkan.ozgen@ae.metu.edu.tr

energy balance and surface water dynamics, [Ruff and Duesterhaus, 1985; Anderson, 2004]. Icing analyses are performed for reference and scaled conditions using a CFD tool ANSYS® Fluent 18.0 with in-flight icing code FENSAP-ICE and in-house icing code AEROMSICE-2D. The ice accretions obtained by analyses are compared with experimental and computational data available in the literature. The scaling method is tested for icing cases provided in [Wright, Gent and Guffond, 1997]. The ice accretions on airfoils NACA0012 and SA13112 are obtained for reference and scaled conditions with computational analyses using an in-house icing code AEROMSICE-2D and a commercial CFD tool ANSYS® Fluent 18.0 and in-flight icing code FENSAP-ICE and ice shapes and collection efficiencies for these conditions for reference and scaled ice accretions are compared.

METHODOLOGY

For in flight icing to occur, supercooled droplets must be present and ambient temperature must be below 0°C. Droplets may freeze instantaneously after impingement and form rime ice or some of the impinging droplets may freeze and some may run downstream and freeze later forming glaze ice. The freezing fraction is the ratio of the amount of water that freezes at impingement to the total amount of impinging water. Thus, the freezing fraction is unity for rime ice and it takes a value of 0 to 1 for glaze ice. The icing type changes the characteristics of ice formation and final ice shape. Rime ice is a dry, opaque ice which usually forms at low airspeed, low temperatures and low liquid water content icing environments. While glaze ice is a wet ice which forms at temperatures around 0°C, and high liquid water content icing environments. Icing cases given in [Wright, Gent and Guffond, 1997] consist of both conditions to obtain rime and glaze ice. Resulting ice shapes of experiments and numerical analyses are provided. To investigate the scaling method, icing conditions of these cases are selected.

Icing Similitude Analysis

A scaling method that produces similar ice accretions for scaled model size and/or test conditions requires the similitudes of geometry, flow field, droplet trajectory, water catch, energy balance and surface water dynamics [Ruff and Duesterhaus, 1985; Anderson, 2004].

For rime ice, since all supercooled droplets that contacts the surface freeze immediately and there is no water film layer, achieving energy balance and surface water dynamics similitudes is not necessary, first four similitudes are enough to achieve ice accretion similarity for rime ice.

Modified Ruff Method [Anderson, 2004], which is a scaling method that is derived from similitude analysis is employed that is the Ruff Method with the addition of surface water dynamics similitude by matching Weber number, We . Assuming that the geometry and flow similarity are achieved, the droplet trajectory similarity, the similarity of the total mass of liquid water hitting the surface, the energy balance similarity and surface-water dynamics similarity shall be ensured for ice accretion similitude. To provide that, modified inertia parameter (K_0), accumulation efficiency (β_0), accumulation parameter (A_c), freezing rate (n_0), and droplet energy transfer parameter (ϕ) and Weber number (We) are to be matched.

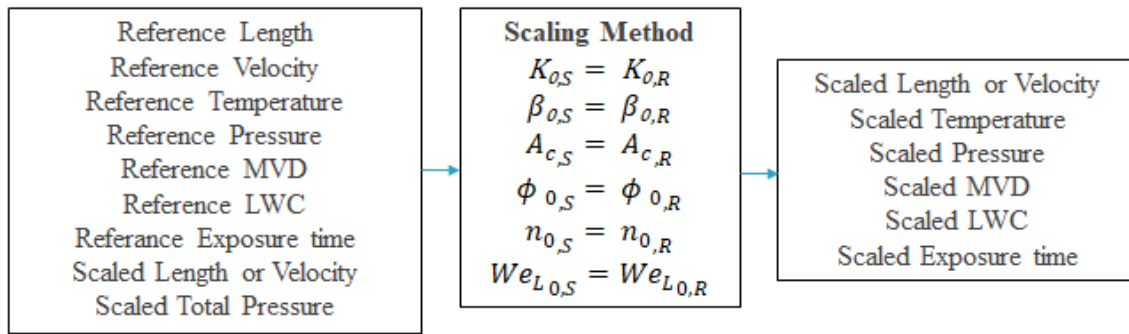


Figure 1: Flow chart for similitude method

Geometric Similarity: The shape and material of scaled geometry and reference geometry should be similar for similar flow and icing physics.

Flow Field Similarity: Flight condition similitude is achieved by matching the Mach Number and Reynolds Number for reference and scaled conditions.

$$M = \frac{V}{\sqrt{\gamma R_a T}} \quad (1)$$

$$Re_a = \frac{V d \rho_a}{\mu_a} \quad (2)$$

However, matching these simultaneously is not feasible considering the parameters constituting these numbers also constitute more critical scaling parameters regarding the droplet trajectory and ice accretion. Thus, for most scaling analyses matching the Mach Number and Reynolds Number is not aimed. This assumption might be justified considering the fact that in majority of the icing conditions, the Mach number is relatively low and compressibility effects are negligible and ice accretion occurs near the stagnation regions where the boundary layer is thin and viscous effects are rather small.

Therefore, the similarity of flow field is considered to be achieved when the Mach number and Reynolds number is in the interval of $M@Re = 2 \times 10^5 < M < M_{critical}$ near the stagnation region, [Ruff and Duesterhaus, 1985]. Lower limit corresponds to a Reynolds number that the velocity distribution is preserved up to stall and upper limit corresponds to critical Mach number where supersonic flow is present.

Drop Trajectory Similarity: Droplet impingement zones and droplet trajectories should be matched for drop trajectory similitude. Modified inertia parameter, K_0 , and collection efficiency, β_0 , should match for drop trajectory similarity.

Collection efficiency is defined as the ratio of the mass of droplets impinges on a body in unit time to the mass of droplets that would impinge if the droplets were following straight line trajectories that is illustrated in Figure 2.

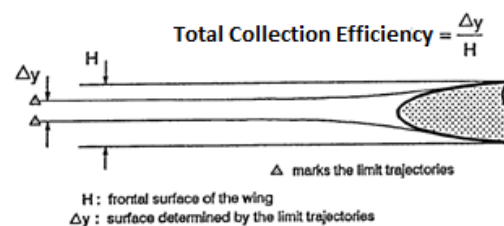


Figure 2: Total collection efficiencies [Paraschivou and Saeed, 2007]

$$K_{0,S} = K_{0,R} \quad (3)$$

$$K_0 = \frac{1}{8} + \frac{\lambda}{\lambda_{Stokes}} \left(K - \frac{1}{8} \right) \quad (4)$$

$$K = \frac{\rho_w (MVD)^2 V}{18 d \mu_a} \quad (5)$$

$$\frac{\lambda}{\lambda_{Stokes}} = \frac{1}{0.8388 + 0.001483 Re_d + 0.1847 \sqrt{Re_d}} \quad (6)$$

$$Re_\delta = \frac{V MVD \rho_a}{\mu_a} \quad (7)$$

$$\beta_0 = \frac{1.40 \left(K_0 - \frac{1}{8} \right)^{0.84}}{1 + 1.40 \left(K_0 - \frac{1}{8} \right)^{0.84}} \quad (8)$$

Water Catch Similarity: The amount of ice accreted depends on the amount of water that impinges the surface. For ice accretion similitude, water catch parameters should match.

$$A_{c,S} = A_{c,R} \quad (9)$$

$$A_c = \frac{LWC V t_{exp}}{\rho_i d} \quad (10)$$

Energy Balance Similarity: Ice accretion occurs when the supercooled droplets hit the air vehicle surface and freezes immediately or a fraction of them freezes and remainders freeze downstream. For the first case, that is the formation of rime ice, there is no need for energy balance similitude since all impinging water freezes at the instant of impingement, at impinging point.

Ice accretes near stagnation point. Thus, without sacrificing accuracy much, energy balance can be calculated along stagnation line.

The energy balance is required for calculating the ratio of water that hits the surface and freezes which is defined as freezing factor (n_0). For rime is the freezing factor is unity. For glaze ice, freezing factor is less than 1, and it is a parameter to be matched for ice accretion similitude. When the freezing factor at stagnation point (n_0) is less than 0, that concludes that ice accretion happens outside of the stagnation point.

$$n_{0,S} = n_{0,R} \quad (11)$$

$$n_0 = \left(\frac{c_{p,ws}}{\Lambda_f} \right) \left(\phi + \frac{\theta}{b} \right) \quad (12)$$

$$b = \frac{LWC V \beta_0 c_{p,ws}}{h_c} \quad (13)$$

$$\phi = T_f - T_{st} - \frac{V^2}{2c_{p,ws}} \quad (14)$$

$$\theta = T_s - T_{st} - \frac{V^2}{2c_{p,a}} + \frac{h_G}{h_c} \Lambda_v \left(\frac{\frac{P_{ww}}{T_{st}} - \frac{P_{tot}}{T_{tot}} \frac{P_w}{P_{st}}}{\frac{1}{0.622} \frac{P_{tot}}{T_{tot}} - \frac{P_{ww}}{T_{st}}} \right) \quad (15)$$

Surface-Water Dynamics Similarity:

For glaze ice a water film is present. The surface water dynamics affects the accreted ice shape. Weber number for reference and scaled conditions should be matched for surface-water dynamic similarity.

$$We_L = \frac{V^2 L \rho_a}{\sigma_{w/a}} \quad (16)$$

Flow Field Solution

The flow field solution is required to obtain velocity and pressure distributions on the airfoil. In-house icing code AEROMSICE-2D employs Hess-Smith panel method [Katz and Plotkin, 2001] coupled with a boundary-layer solver, further information is provided in [Özgen and Canıbek, 2009].

Commercial software ANSYS® Fluent 18.0 obtains the flow field solution by solving Reynolds Averaged Navier Stokes Equations by a finite volume method (FVM) for the spatial discretization. Turbulence is modeled with two equation k- ω SST turbulence model. The flow field solution is provided to the in-flight icing code FENSAP-ICE.

Droplet Trajectories and Collection Efficiencies

In-house icing code AEROMSICE-2D solves droplet trajectories by utilizing Lagrangian approach that refers to tracking each droplet released from the far field. The theory and calculations of droplet trajectories are presented in [Özgen and Canıbek, 2009].

Droplet trajectories are calculated in FENSAP-ICE DROP3D module by utilizing Eulerian approach that obtains the properties of droplets in the flow at the nodes of the discretized flow domain. The method is employing Eulerian two-fluid model that is Navier-Stokes equations with the addition of droplets to the continuity and momentum equations. Theory and calculations are further explained in [Bourgault, Habashi, Dompierre, Boutanios and Di Bartolomeo, 1997].

Thermodynamic Analysis and Icing Prediction

In-house icing code AEROMSICE-2D obtains convective heat transfer coefficients from two-dimensional integral boundary layer method mentioned in flow field solution part to perform the thermodynamic analysis. Extended Messinger Model that is introduced in [Myers, 2001] is employed for the ice accretion solution. Further information about, thermodynamic and ice accretion calculations is provided in [Özgen and Canıbek, 2009].

FENSAP-ICE receives frictional forces and heat fluxes from the viscous flow solution that is provided by ANSYS® Fluent 18.0 flow solver. Thus, for ice accretion calculations heat transfer coefficient is obtained from the convective heat transfer calculated by the flow solver. Ice accretion computations in FENSAP-ICE software are performed in ICE3D module. The frictional forces and heat fluxes are imported from the viscous flow solution provided by ANSYS® Fluent 18.0 and the water volume fraction provided by DROP3D. Ice accretion is modeled by modifying classical Messinger model introduced in [Messinger, 1953] into partial

differential equations. Theory and calculations are further explained in [Bourgault, Beaugendre and Habashi, 2000]

RESULTS AND DISCUSSION

Size and velocity scaling are performed for icing cases provided in [Wright, Gent and Guffond, 1997] for airfoils NACA0012 and SA13112. The ice shapes and collection efficiencies for cases with airfoil NACA0012 are obtained for by AEROMSICE-2D, in-house icing code, and FENSAP-ICE software. For these cases size-scaling of $\frac{1}{2}$ is performed on the reference conditions.

For airfoil SA13112, ice shapes and collection efficiencies are obtained by FENSAP-ICE software. For these cases, velocity scaling to obtain lower test velocities is performed on reference conditions. For simplicity of obtaining geometry and mesh for the solution, the velocities are scaled by model size scaling of 2. When the test velocity is decreased, the size of the scaled model increases and vice versa. Since the velocity for scaled model is inversely proportional to size of the scaled model to match the surface-water dynamics, Weber number. The MVD and the exposure time decreases to compensate the shrinkage of the geometry and to match the total water catch. The rest of the parameters are balanced by the relations of scaling equations.

Agreement of final ice shapes and collection efficiencies are compared for 16 cases given in [Wright, Gent and Guffond, 1997] that are listed in APPENDIX and an additional case.

Ice accretions obtained for cases 27, 28, 29, 30, 31, 32 whose conditions given in Table 1 to 6 and ice shapes given in Figure 3 to Figure 8 shows good agreement with experiment for both reference and scaled cases. The reference and scaled ice shapes obtained by FENSAP-ICE and AEROMSICE-2D well-matched among reference and scaled cases and among solvers. The collection efficiencies are overlapping especially for lower surface with a slight difference in upper surface.

Table 1: Case 27 icing conditions for reference and scaled cases in reference [Wright, Gent and Guffond, 1997]

Case	Type	c, m	Tst, °C	V, m/s	MVD, μm	LWC, g/m^3	t _{exp} , s	P _{sr} , (kPa)	K ₀	β_0	A _c	n ₀	b	Φ , K	θ , K	Re _a , 10 ⁴	We _L , 10 ⁶
27	Ref.	0.53	-27.80	58.10	20.00	1.30	480.00	95.610	1.81	0.68	2.36	1.13	0.55	27.55	34.07	8.39	0.87
	Scaled	0.265	-28.20	82.17	11.44	1.48	149.54	95.341	1.81	0.68	2.36	1.13	0.53	27.55	32.70	5.93	0.87

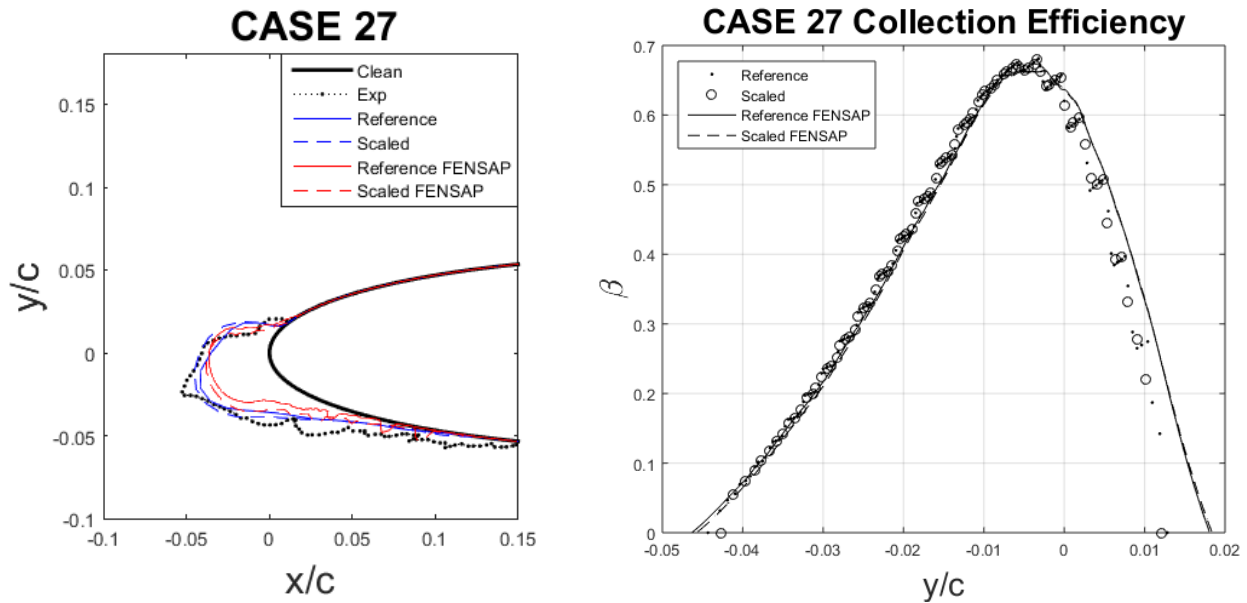


Figure 3: Case 27 ice shapes and collection efficiencies in reference [Wright, Gent and Guffond, 1997]

Ice accretions obtained for Case 28 whose conditions given in Table 2 and ice shapes given in Figure 4 shows good agreement however there is a horn in AEROMSICE-2D scaled ice shape that is not present for experimental data and results of other analysis.

Table 2: Case 28 icing conditions for reference and scaled cases in reference [Wright, Gent and Guffond, 1997]

Case	Type	c, m	Tst, °C	V, m/s	MVD, μm	LWC, g/m ³	t _{exp} , s	P _s , (kPa)	K ₀	β ₀	A _c	n ₀	b	Φ, K	θ, K	Re _a , 10 ⁴	We _L , 10 ⁶
28	Ref.	0.53	-19.80	58.10	20.00	1.30	480.00	95.610	1.80	0.68	2.36	0.82	0.56	19.55	25.21	7.92	0.87
	Scaled	0.265	-20.20	82.17	11.45	1.46	151.39	95.484	1.80	0.68	2.36	0.82	0.53	19.55	23.86	5.61	0.87

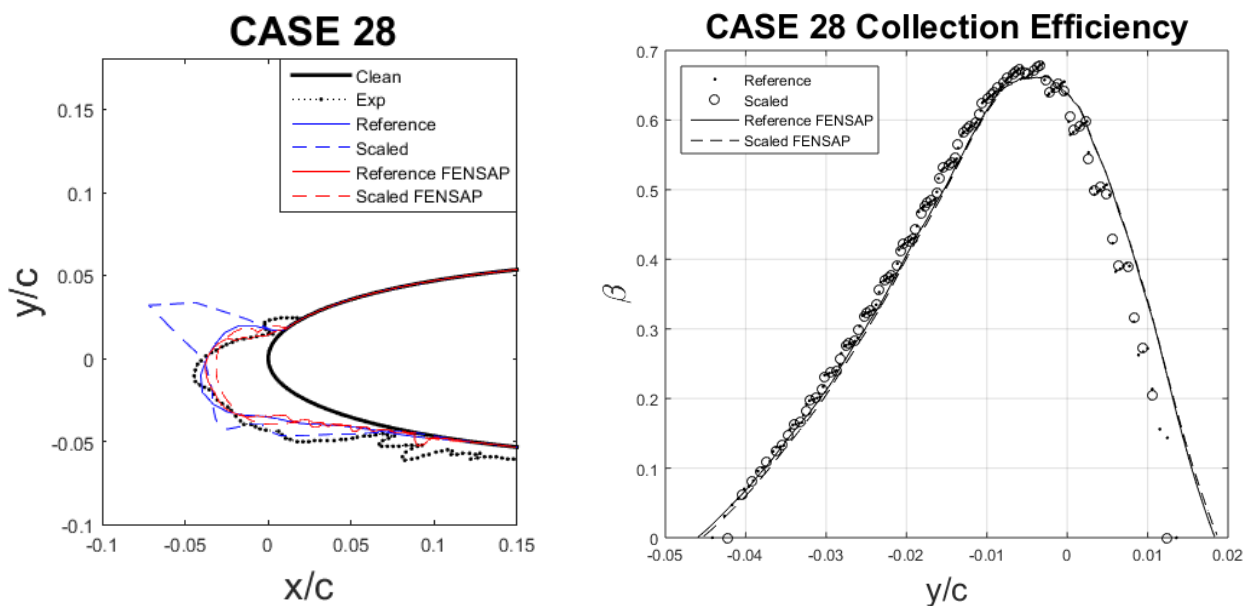


Figure 4: Case 28 ice shapes and collection efficiencies in reference [Wright, Gent and Guffond, 1997]

For ice accretions given in Figure 5 for Case 29 whose conditions given in Table 3 shows good agreement with experiment for reference case, for scaled case the horn angle is not well predicted by AEROMSICE-2D.

Table 3: Case 29 icing conditions for reference and scaled cases in reference [Wright, Gent and Guffond, 1997]

Case	Type	c, m	Tst, °C	V, m/s	MVD, μm	LWC, g/m ³	t _{exp} , s	P _{sr} (kPa)	K ₀	β ₀	A _c	n ₀	b	Φ, K	θ, K	Re _a , 10 ⁴	We _L , 10 ⁶
29	Ref.	0.53	-13.90	58.10	20.00	1.30	480.00	95.610	1.79	0.68	2.36	0.58	0.56	13.65	18.18	7.60	0.87
	Scaled	0.265	-14.30	82.17	11.46	1.43	154.26	95.584	1.79	0.68	2.36	0.58	0.52	13.65	16.85	5.39	0.87

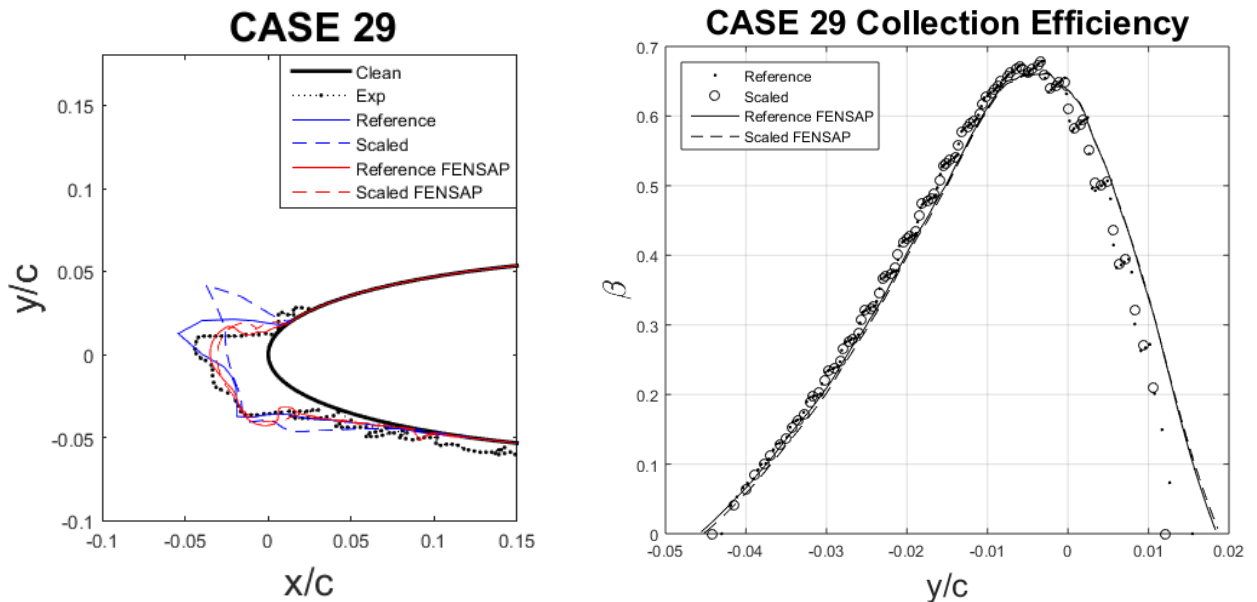


Figure 5: Case 29 ice shapes and collection efficiencies in reference [Wright, Gent and Guffond, 1997]

For ice accretions given in Figure 6 to Figure 8 for Case 30 to 32 whose conditions given in Table 4 to 6 shows good agreement with experiment for both reference and scaled cases. AEROMSICE-2D slightly overpredicts the horn geometry while FENSAP-ICE underpredicts it.

Table 4: Case 30 icing conditions for reference and scaled cases in reference [Wright, Gent and Guffond, 1997]

Case	Type	c, m	Tst, °C	V, m/s	MVD, μm	LWC, g/m ³	t _{exp} , s	P _{sr} (kPa)	K ₀	β ₀	A _c	n ₀	b	Φ, K	θ, K	Re _a , 10 ⁴	We _L , 10 ⁶
30	Ref.	0.53	-6.70	58.10	20.00	1.30	480.00	95.610	1.79	0.68	2.36	0.27	0.57	6.45	8.66	7.24	0.87
	Scaled	0.265	-7.10	82.17	11.46	1.32	166.81	95.700	1.79	0.68	2.36	0.27	0.49	6.45	7.40	5.14	0.87

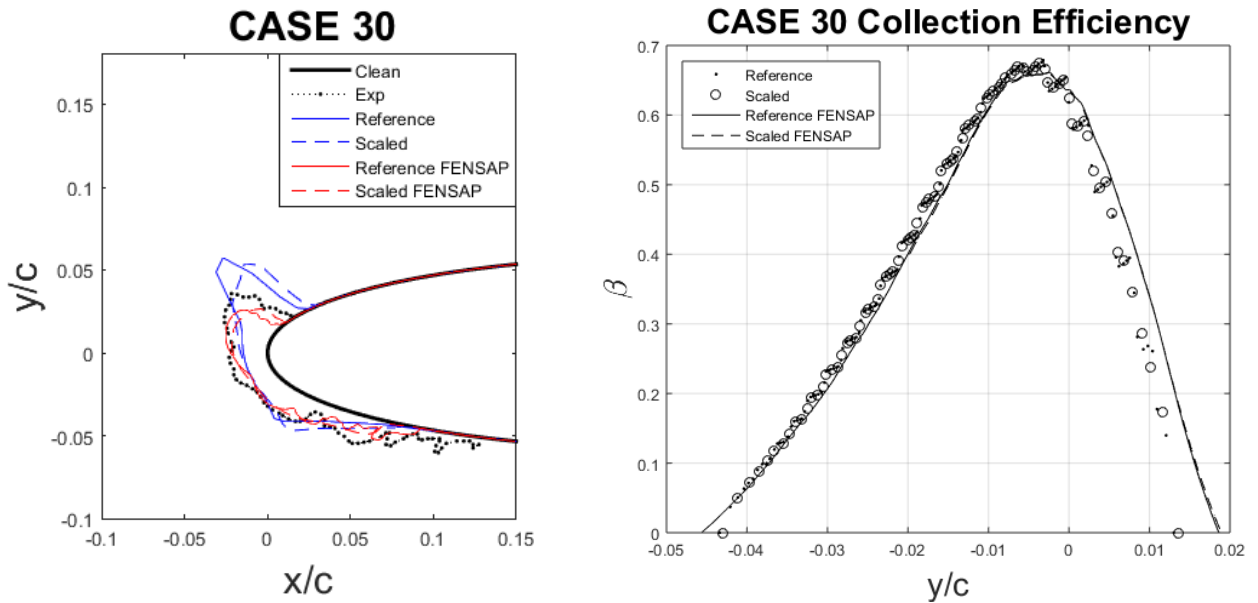


Figure 6: Case 30 ice shapes and collection efficiencies in reference [Wright, Gent and Guffond, 1997]

Table 5: Case 31 icing conditions for reference and scaled cases in reference [Wright, Gent and Guffond, 1997]

Case	Type	c , m	T_{st} , °C	V , m/s	MVD, μm	LWC, g/m^3	t_{exp} , s	P_s , (kPa)	K_0	β_0	A_c	n_0	b	Φ , K	θ , K	Re_a , 10^4	We_L , 10^6
31	Ref.	0.53	-3.90	58.10	20.00	1.30	480.00	95.610	1.78	0.68	2.36	0.15	0.57	3.65	4.58	7.10	0.87
	Scaled	0.265	-4.30	82.17	11.47	1.13	195.64	95.744	1.78	0.68	2.36	0.15	0.42	3.65	3.36	5.04	0.87

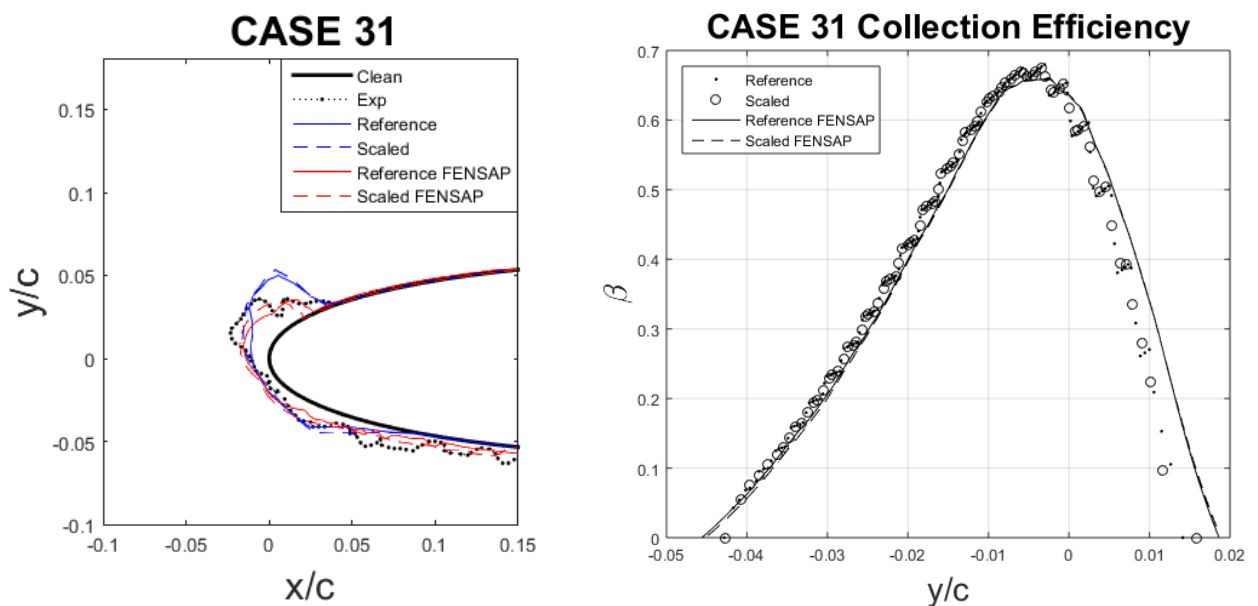


Figure 7: Case 31 ice shapes and collection efficiencies in reference [Wright, Gent and Guffond, 1997]

Table 6: Case 32 icing conditions for reference and scaled cases in reference [Wright, Gent and Guffond, 1997]

Case	Type	c, m	Tst, °C	V, m/s	MVD, μm	LWC, g/m ³	t _{exp} , s	P _s , (kPa)	K ₀	β ₀	A _c	n ₀	b	Φ, K	θ, K	Re _a , 10 ⁴	We _L , 10 ⁶
32	Ref.	0.53	-2.80	58.10	20.00	1.30	480.00	95.610	1.78	0.68	2.36	0.10	0.57	2.55	2.91	7.05	0.87
	Scaled	0.265	-3.20	82.17	11.47	0.85	259.89	95.761	1.78	0.68	2.36	0.10	0.31	2.55	1.70	5.01	0.87

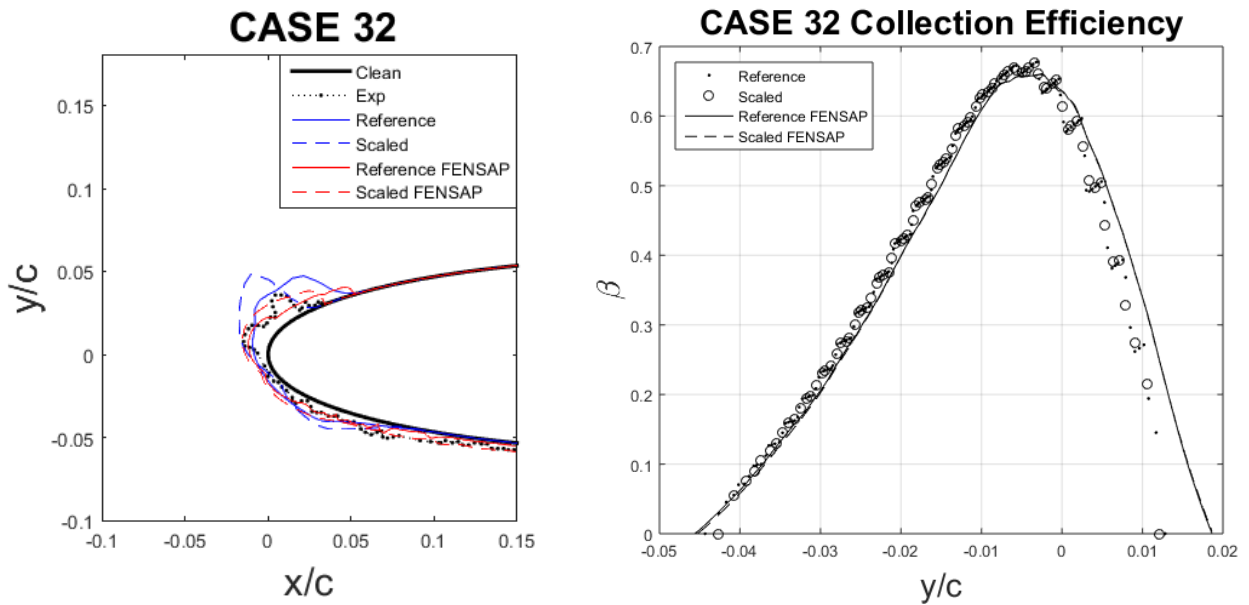


Figure 8: Case 32 ice shapes and collection efficiencies in reference [Wright, Gent and Guffond, 1997]

For ice accretions given in Figure 9 for Case 33 whose conditions given in Table 7, both AEROMSICE-2D and FENSAP-ICE underpredicts ice height. While there is a good agreement between scaled and reference ice shapes for AEROMSICE-2D, FENSAP-ICE ice shape obtained for scaled case is not well-matched with reference ice shape.

Table 7: Case 33 icing conditions for reference and scaled cases in reference [Wright, Gent and Guffond, 1997]

Case	Type	c, m	Tst, °C	V, m/s	MVD, μm	LWC, g/m ³	t _{exp} , s	P _s , (kPa)	K ₀	β ₀	A _c	n ₀	b	Φ, K	θ, K	Re _a , 10 ⁴	We _L , 10 ⁶
33	Ref.	0.53	-30.50	93.89	20.00	1.05	372.00	92.060	2.43	0.74	2.39	1.07	0.62	29.60	34.30	13.32	2.27
	Scaled	0.265	-31.55	132.78	11.27	1.10	125.03	88.256	2.43	0.74	2.39	1.07	0.56	29.60	30.97	9.10	2.27

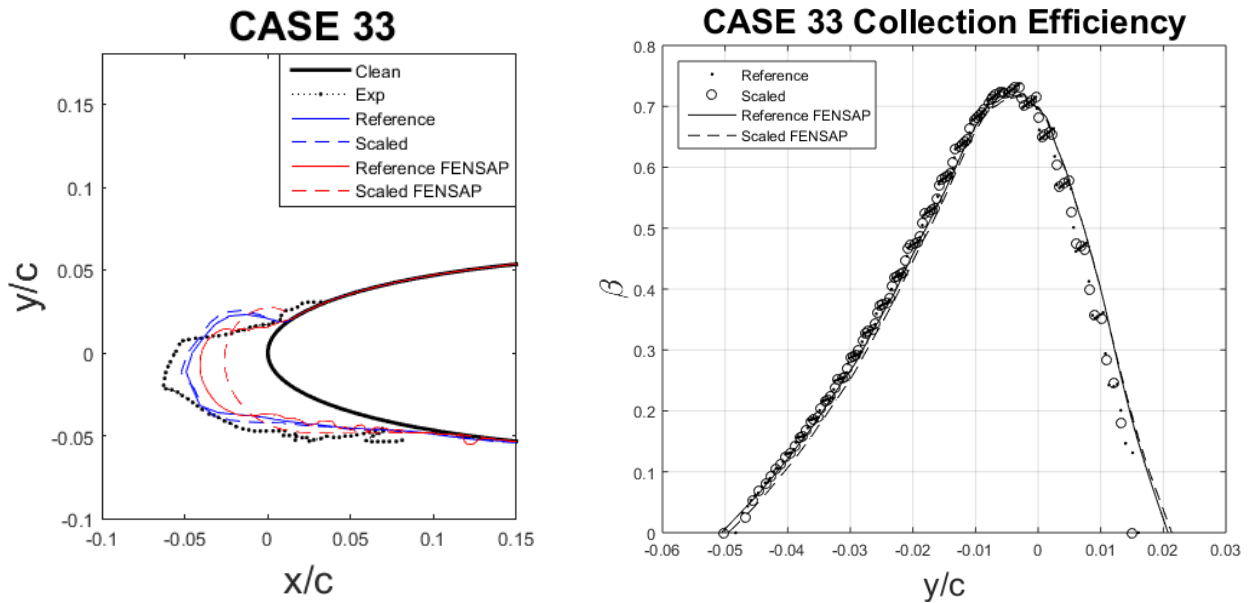


Figure 9: Case 33 ice shapes and collection efficiencies in reference [Wright, Gent and Guffond, 1997]

For ice accretions given in Figure 10 for Case 34 whose conditions given in Table 8 shows AERMSICE-2D overpredict the horn shape and angle while FENSAP-ICE underpredicts the horn shape.

Table 8: Case 34 icing conditions for reference and scaled cases in reference [Wright, Gent and Guffond, 1997]

Case	Type	c, m	Tst, °C	V, m/s	MVD, μm	LWC, g/m ³	t _{exp} , s	P _s , (kPa)	K ₀	β ₀	A _c	n ₀	b	Φ, K	θ, K	Re _a , 10 ⁴	We _L , 10 ⁶
34	Ref.	0.53	-16.60	93.89	20.00	1.05	372.00	92.060	2.42	0.74	2.39	0.57	0.64	15.70	18.77	12.05	2.27
	Scaled	0.265	-17.65	132.78	11.31	1.01	136.28	88.848	2.42	0.74	2.39	0.57	0.52	15.70	15.49	8.29	2.27

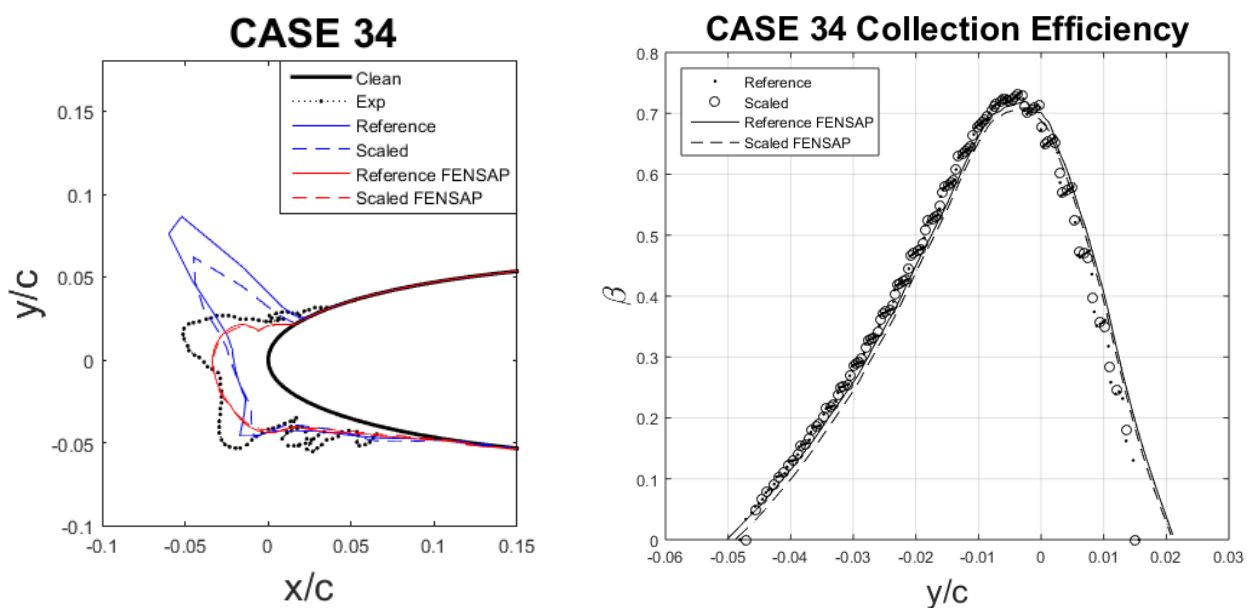


Figure 10: Case 34 ice shapes and collection efficiencies in reference [Wright, Gent and Guffond, 1997]

For ice accretions given in Figure 11 for Case 35 whose conditions given in Table 9 shows good agreement with experiment for both reference and scaled cases but final ice shapes obtained by AEROMSICE-2D overpredict the horn shape and angle.

Table 9: Case 35 icing conditions for reference and scaled cases in reference [Wright, Gent and Guffond, 1997]

Case	Type	c, m	Tst, °C	V, m/s	MVD, μm	LWC, g/m ³	t _{exp} , s	P _s , (kPa)	K ₀	β ₀	A _c	n ₀	b	Φ, K	θ, K	Re _a , 10 ⁴	We _L , 10 ⁶
35	Ref.	0.53	-12.20	93.89	20.00	1.05	372.00	92.060	2.42	0.74	2.39	0.41	0.64	11.30	13.30	11.69	2.27
	Scaled	0.265	-13.25	132.78	11.31	0.93	149.29	89.023	2.42	0.74	2.39	0.41	0.48	11.30	10.07	8.05	2.27

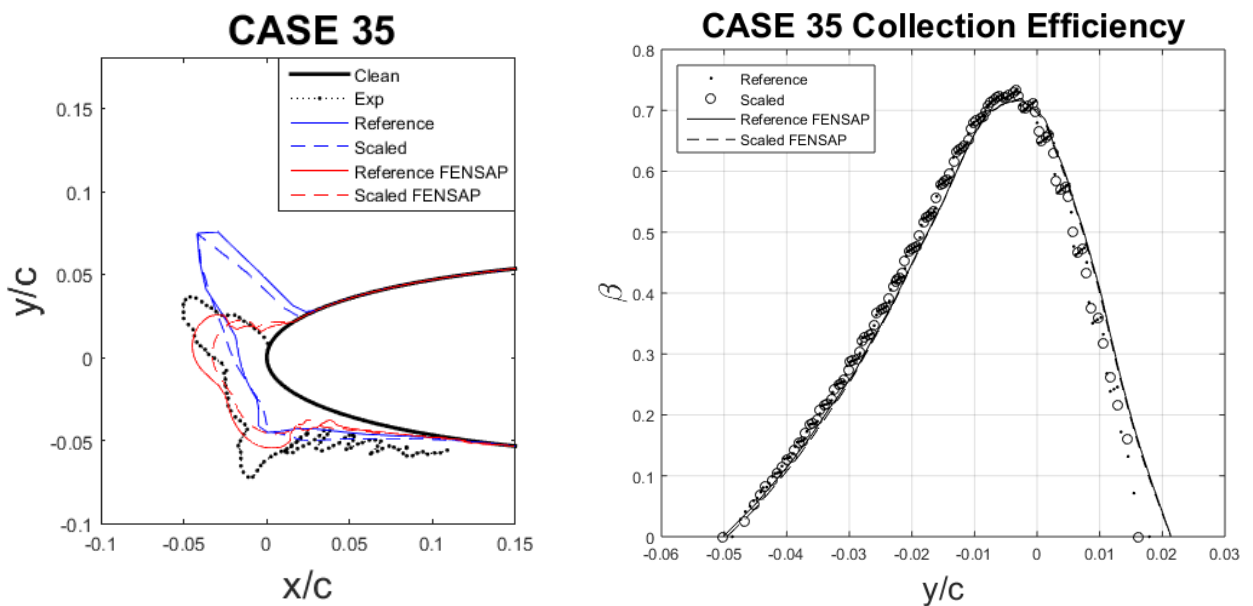


Figure 11: Case 35 ice shapes and collection efficiencies in reference [Wright, Gent and Guffond, 1997]

For ice accretions given in Figure 12 for Case 36 whose conditions given in Table 10 shows reference ice shape upper limit is overpredicted and scaled ice shape horn height is overpredicted by AEROMSICE-2D and ice thickness for scaled ice shape is overpredicted and ice horn shapes are underpredicted for reference case by FENSAP-ICE.

Table 10: Case 36 icing conditions for reference and scaled cases in reference [Wright, Gent and Guffond, 1997]

Case	Type	c, m	Tst, °C	V, m/s	MVD, μm	LWC, g/m ³	t _{exp} , s	P _s , (kPa)	K ₀	β ₀	A _c	n ₀	b	Φ, K	θ, K	Re _a , 10 ⁴	We _L , 10 ⁶
36	Ref.	0.53	-6.60	93.89	20.00	1.05	372.00	92.060	2.42	0.74	2.39	0.18	0.64	5.70	5.72	11.25	2.27
	Scaled	0.265	-7.65	132.78	11.33	0.38	367.67	89.238	2.42	0.74	2.39	0.24	0.20	5.70	2.56	7.77	2.27

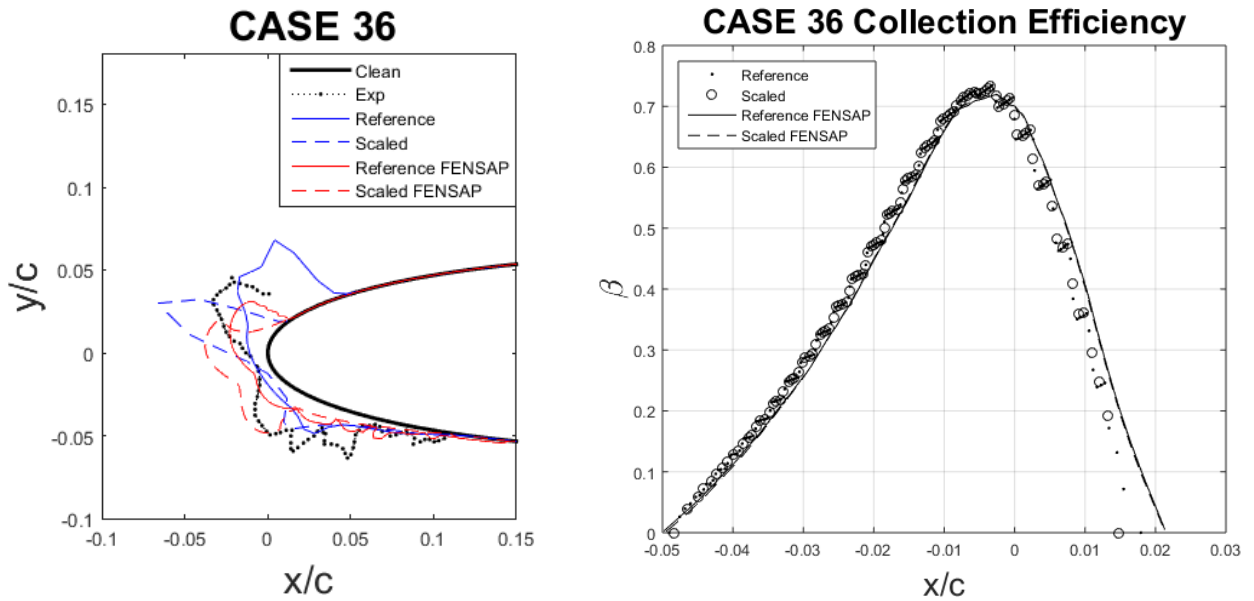


Figure 12: Case 36 ice shapes and collection efficiencies in reference [Wright, Gent and Guffond, 1997]

For ice accretions given in Figure 13 and Figure 14 for Case 37 and 38 whose conditions given in Table 11 do not show good agreement with experiment for both reference and scaled cases. Although the ice shapes are well-matched for both solvers AEROMSICE-2D and FENSAP-ICE for both reference and scaled ice shapes, the amount, shape and limits of ice obtained from experiment is contrasting.

Table 11: Case 37 and 38 icing conditions for reference and scaled cases in reference [Wright, Gent and Guffond, 1997]

Case	Type	c, m	Tst, °C	V, m/s	MVD, μm	LWC, g/m ³	t _{exp} , s	P _s , (kPa)	K ₀	β ₀	A _c	n ₀	b	Φ, κ	θ, κ	Re _a , 10 ⁴	We _L , 10 ⁶
37 & 38	Ref.	0.53	-12.30	130.50	17.50	0.50	120.00	90.500	2.40	0.74	0.51	0.45	0.36	10.43	9.09	15.98	4.39
	Scaled	0.265	-14.32	184.55	9.67	0.06	376.29	80.080	2.40	0.74	0.51	1.24	0.04	10.43	3.17	10.14	4.39

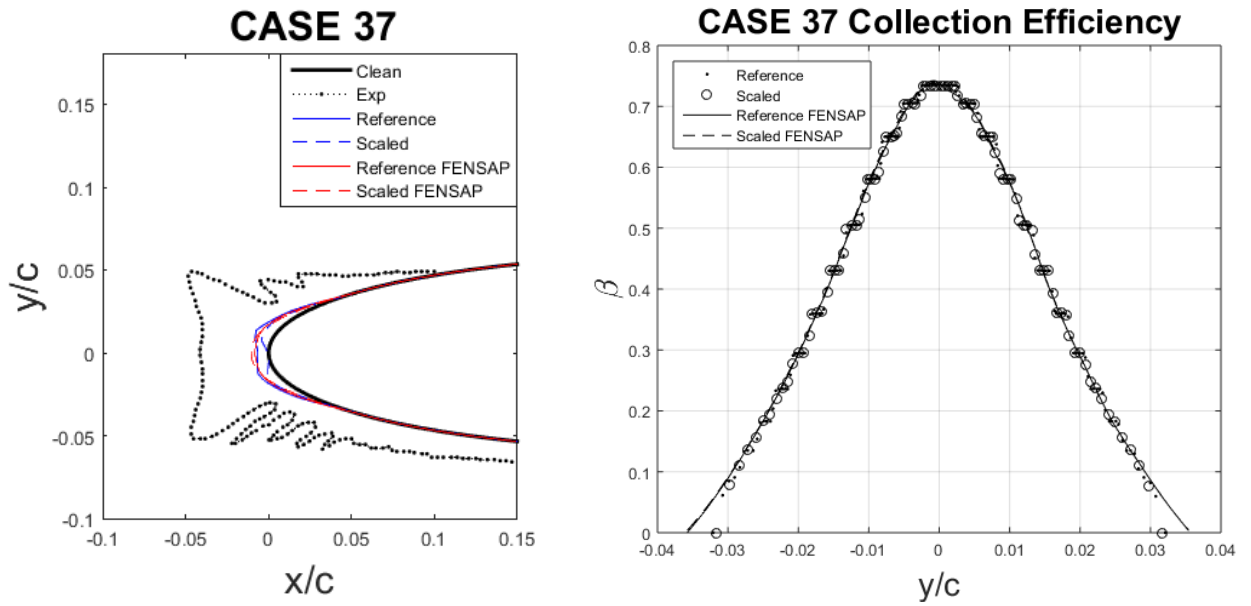


Figure 13: Case 37 ice shapes and collection efficiencies in reference [Wright, Gent and Guffond, 1997]

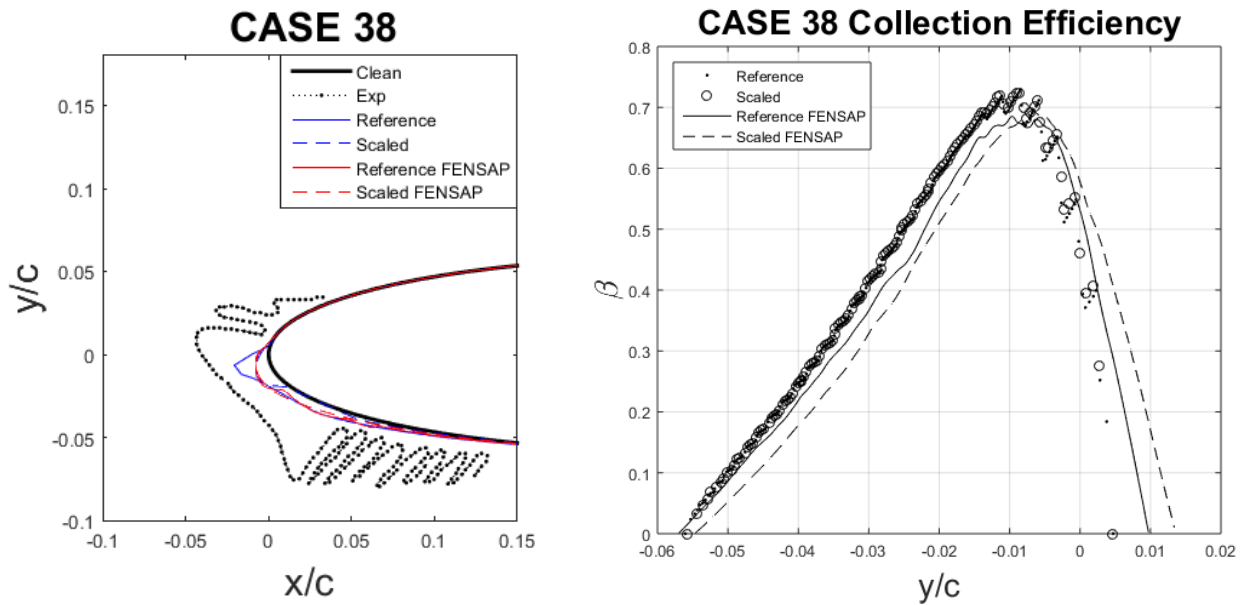


Figure 14: Case 38 ice shapes and collection efficiencies in reference [Wright, Gent and Guffond, 1997]

For ice accretions given in

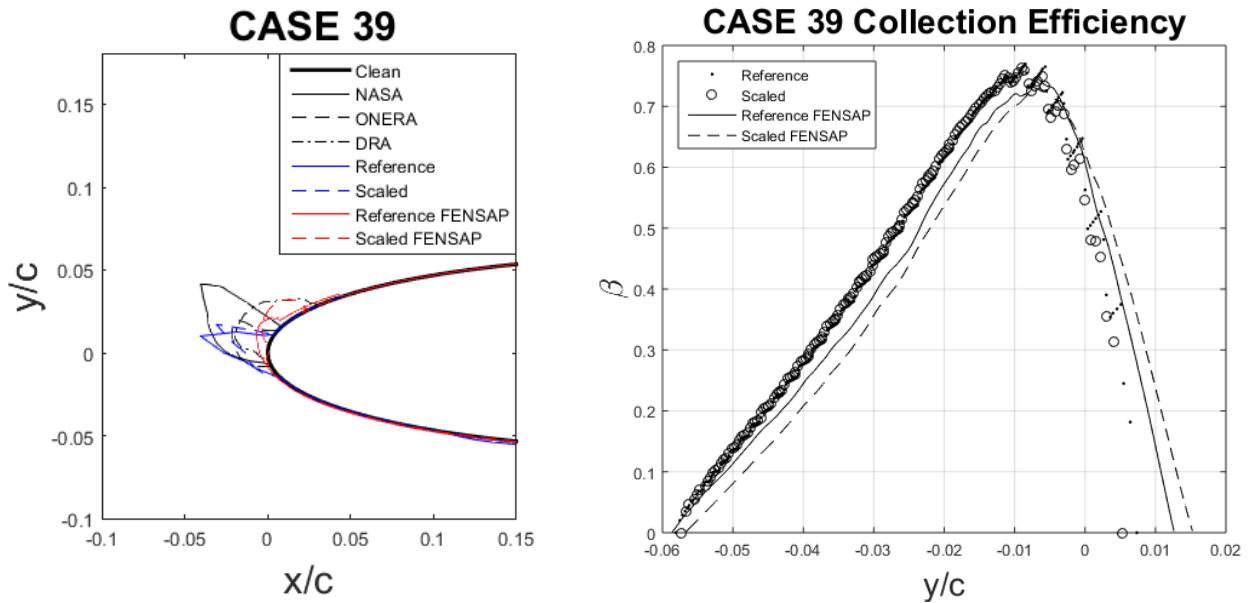


Figure 15 for Case 39 whose conditions given in Table 12 there is no available experimental result. Thus, when the results of current study are compared with numerical results in the literature. The ice shape characteristics resemble, however; DRA and FENSAP-ICE obtain circular, smoother ice shapes, whereas, NASA, ONERA and AEROMSICE-2D obtain pointy, sharper ice shapes. The reference and scaled results are in good agreement among each other.

Table 12: Case 39 icing conditions for reference and scaled cases in reference [Wright, Gent and Guffond, 1997]

Case	Type	c, m	Tst, °C	V, m/s	MVD, μm	LWC, g/m ³	t _{exp} , s	P _s , (kPa)	K ₀	β ₀	A _c	n ₀	b	Φ, K	θ, K	Re _{a3} , 10 ⁴	We _L , 10 ⁶
39	Ref.	0.53	-3.90	131.50	20.00	0.60	180.00	85.000	3.03	0.77	0.92	-0.05	0.48	2.00	-2.68	14.29	4.45
	Scaled	0.265	-5.95	185.97	11.22	2.94	13.00	80.360	3.03	0.77	0.92	-0.03	2.02	2.00	-8.73	9.69	4.45

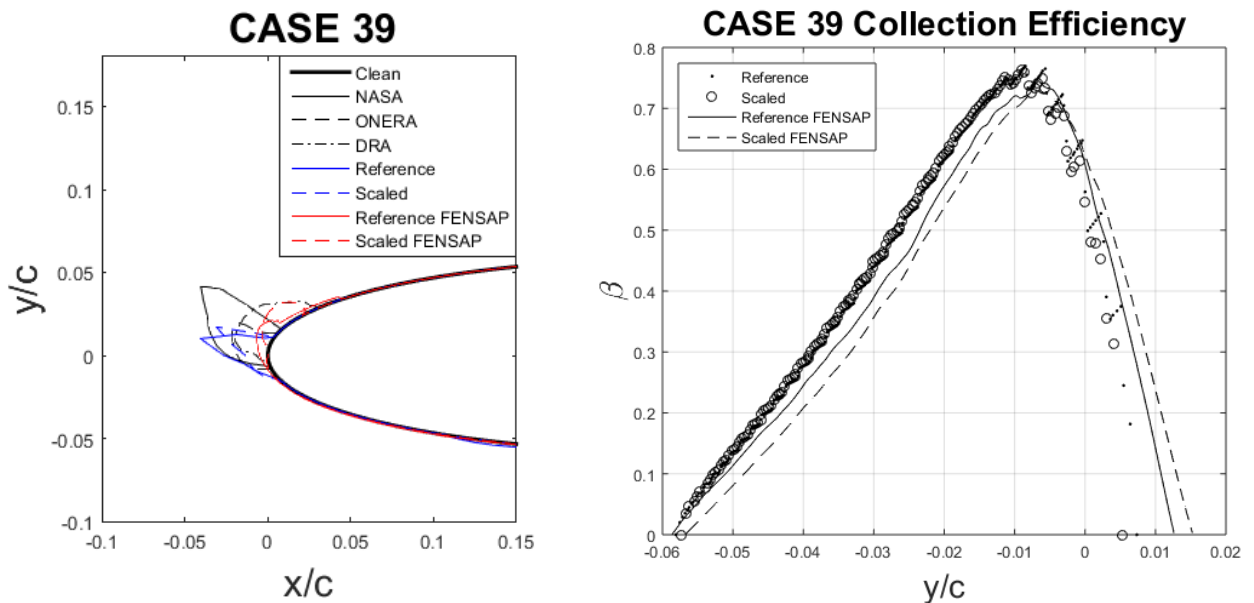


Figure 15: Case 39 ice shapes and collection efficiencies in reference [Wright, Gent and Guffond, 1997]

For the cases given for SA13112 airfoil, the main focus is on velocity scaling. The size for scaled geometry is increasing to match the surface-water dynamics, Weber number. The MVD and the exposure time increases to compensate the growth of the geometry and to match the total water catch. The rest of the parameters are balanced by the relations of scaling equations.

For ice accretions given in Figure 16 for Case 40 whose conditions given in Table 13, the final ice shapes obtained by NASA, ONERA and FENSAP-ICE are well-matched. DRA overpredicts the ice accretion compared to other numerical analyses results, however, still the ice shapes are similar. Reference and scaled ice shapes are also in good agreement among each other, however, neither limits of experimental ice nor its shape match the numerical results.

Table 13: Case 40 icing conditions for reference and scaled cases in reference [Wright, Gent and Guffond, 1997]

Case	Type	c, m	Tst, °C	V, m/s	MVD, μm	LWC, g/m ³	t _{exp} , s	P _s , (kPa)	K ₀	β ₀	A _c	n ₀	b	Φ, K	θ, K	Re _a , 10 ⁴	We _L , 10 ⁶
40	Ref.	0.6	-10.00	81.30	20.00	0.50	900.00	79.500	2.08	0.71	2.10	0.62	0.31	9.37	12.36	9.7	1.93
	Scaled	1.2	-9.61	57.49	36.88	0.47	2682.87	97.85	2.08	0.71	2.10	0.62	0.32	9.37	12.59	16.9	1.93

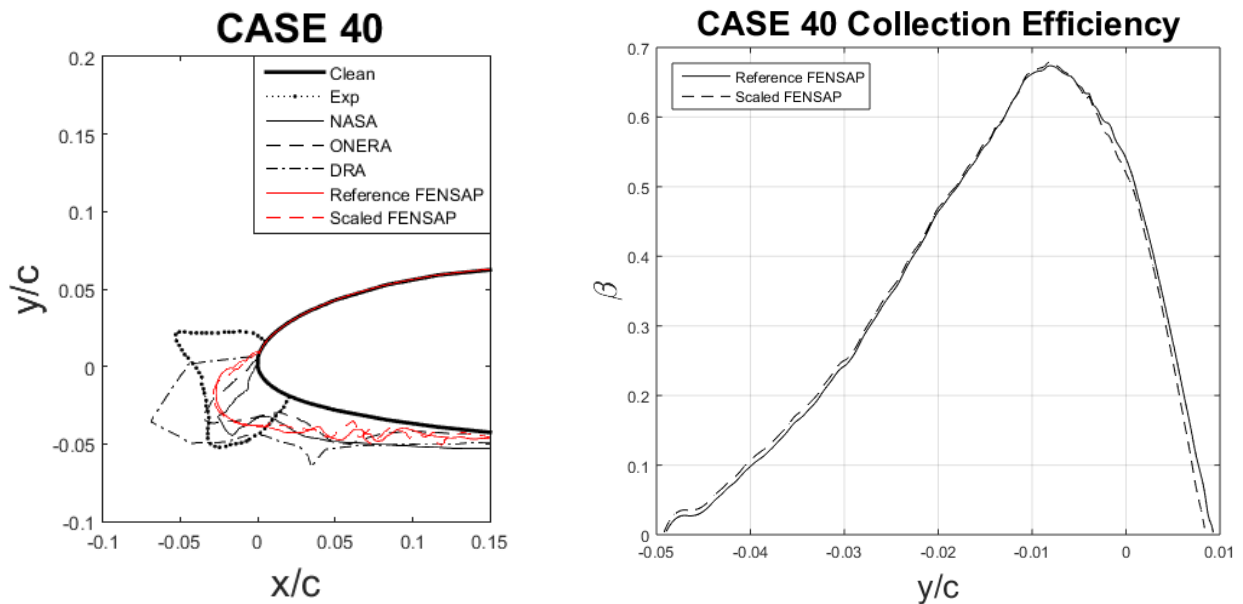


Figure 16: Case 40 ice shapes and collection efficiencies in reference [Wright, Gent and Guffond, 1997]

For ice accretions given in Figure 17 for Case 41 whose conditions given in Table 14, the ice height and limits of ice obtained by FENSAP-ICE are similar to experimental ice. However, the horns are underpredicted for both scaled and reference cases.

Table 14: Case 41 icing conditions for reference and scaled cases in reference [Wright, Gent and Guffond, 1997]

Case	Type	c, m	Tst, °C	V, m/s	MVD, μm	LWC, g/m ³	t _{exp} , s	P _s , (kPa)	K ₀	β ₀	A _c	n ₀	b	Φ, K	θ, K	Re _a , 10 ⁴	We _L , 10 ⁶
------	------	------	---------	--------	---------	-----------------------	----------------------	------------------------	----------------	----------------	----------------	----------------	---	------	------	-----------------------------------	-----------------------------------

41	Ref.	0.6	-10.00	162.50	20.00	0.50	450.00	79.500	3.11	0.78	2.10	0.13	0.49	7.02	1.60	19.49	7.70
	Scaled	1.2	-8.43	114.90	36.77	1.12	570.75	91.772	3.11	0.78	2.10	0.15	1.20	7.02	5.94	31.48	7.70

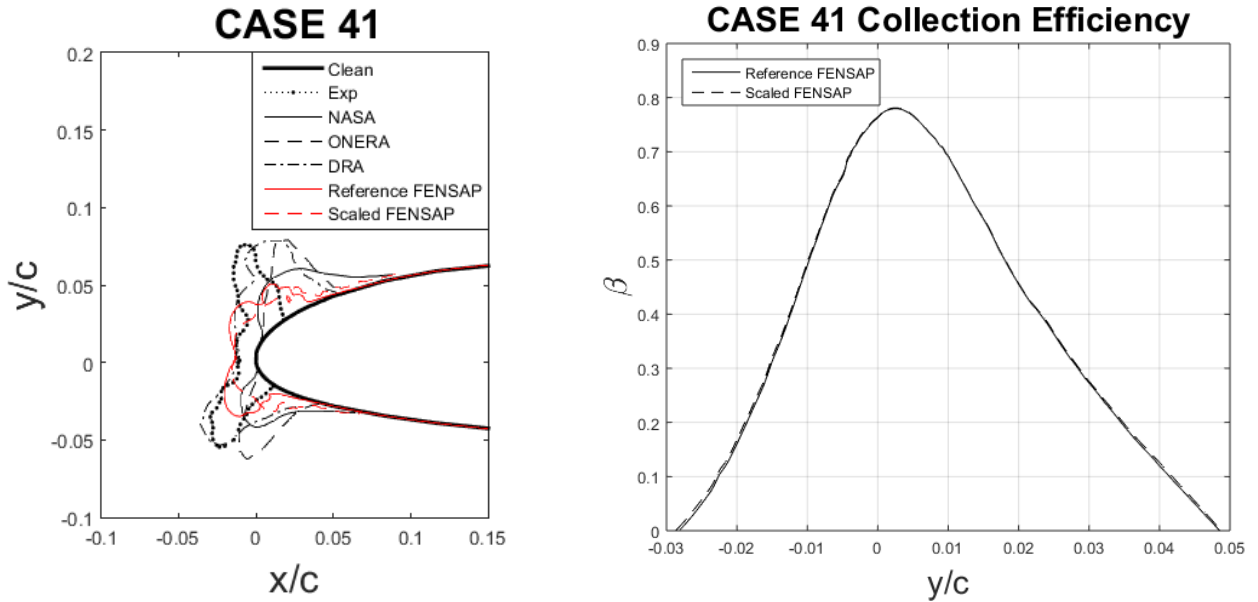


Figure 17: Case 41 ice shapes and collection efficiencies in reference [Wright, Gent and Guffond, 1997]

For ice accretions given in Figure 18 for Case 42 whose conditions given in Table 15, there is no experimental results available but numerical results in the literature are presented. The ice limits of all ice shapes obtained by numerical analyses are similar. The ice height obtained by FENSAP-ICE is well matched with ice shape obtained by NASA. The scaled and reference ice shapes obtained by FENSAP-ICE are also in good agreement.

Table 15: Case 42 icing conditions for reference and scaled cases in reference [Wright, Gent and Guffond, 1997]

Case	Type	c, m	Tst, °C	V, m/s	MVD, μm	LWC, g/m ³	t _{exp} , s	P _s , (kPa)	K ₀	β ₀	A _c	n ₀	b	Φ, K	θ, K	Re _a , 10 ⁴	We _L , 10 ⁶
42	Ref.	0.600	-30.2	249.90	20.0	0.50	180	79.500	3.919	0.811	1.294	0.413	0.610	22.747	6.053	34.53	18.22
	Scaled	1.200	-26.4	176.71	35.7	0.96	266	80.750	3.919	0.811	1.294	0.458	1.387	22.747	18.703	48.28	18.22

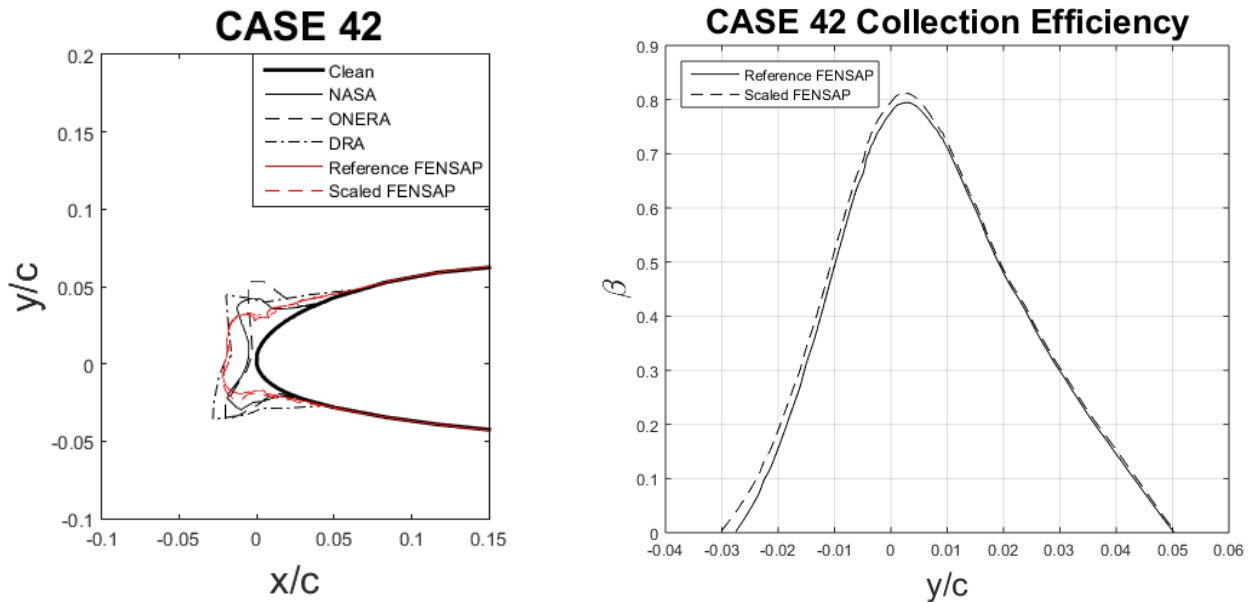


Figure 18: Case 42 ice shapes and collection efficiencies in reference [Wright, Gent and Guffond, 1997]

For ice accretions given in Figure 19 for Case * whose conditions given in Table 16, there is no experimental results available and numerical results in the literature. The case is chosen as a challenging velocity scaling case. The scaled and reference ice shapes and limits obtained by FENSAP-ICE are in good agreement.

Table 16: Case * icing conditions for reference and scaled cases

Case	Type	c, m	Tst, °C	V, m/s	MVD, μm	LWC, g/m ³	t _{exp} , s	P _s , (kPa)	K ₀	β ₀	A _c	n ₀	b	Φ, K	θ, K	Re _a , 10 ⁴	We _L , 10 ⁶
*	Ref.	0.533	-10.0	243.90	20.0	0.12	900	54.890	5.112	0.844	1.705	-1.038	0.176	2.948	-14.915	17.92	15.41
	Scaled	0.800	-7.6	199.08	30.9	0.08	2519	77.820	5.111	0.844	1.705	-1.026	0.108	2.948	-9.042	30.63	15.41

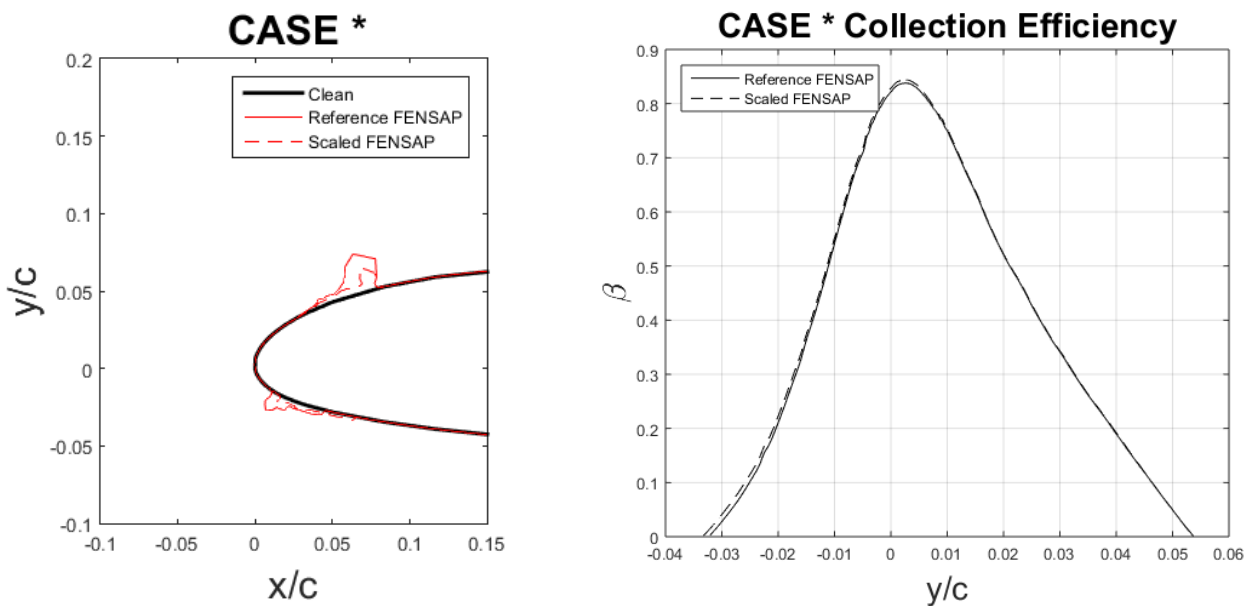


Figure 19: Case * ice shapes and collection efficiencies

CONCLUSIONS

An icing scaling method that is known as modified Ruff method is utilized for scaling several cases having APPENDIX-C icing conditions to obtain similar ice shapes for reference and scaled cases. Both size scaling and velocity scaling is implemented.

The in-house icing code AEROMSICE-2D and commercial icing software FENSAP-ICE are employed for numerical analyses and the resulting ice shapes and collection efficiencies are compared with the experimental and numerical data in the literature.

The collection efficiencies obtained for both numerical tools show good agreement even though the solution method for flow field and droplet trajectory are different.

The ice shapes for scaled and reference conditions obtained by the same solver usually well-matched. The resulting ice shapes obtained by AEROMSICE-2D and FENSAP-ICE also have good agreement, however, AEROMSICE-2D usually overpredicts the horns and FENSAP-ICE underpredicts and smoothens the horns.

The numerical results obtained in current study by both numerical tools show good agreement with experimental and numerical data in literature with a few exceptions. The cases that does not have good matching are usually glaze ice cases that ice shapes are hard to predict. Since glaze ice have more complex icing physics, the prediction and scaling of ice shapes are both challenging.

The success of scaling method for cases that have 3D effects such as swept wings and cases including heating systems are to be investigated for future studies.

References

- Anderson, D. N. (2004) *Manual of Scaling Method*, Technical Report, March 2004.
- Bourgault, Y., Beaugendre, H. and Habashi, W.G. (2000) *Development of a Shallow Water Icing Model in FENSAP-ICE*, Journal of Aircraft, 37, pp. 640-646.
- Bourgault, Y., Habashi, W., Dompierre, J., Boutanios, Z., Di Bartolomeo, W. (1997) *An Eulerian approach to supercooled droplets impingement calculations*. In 35th Aerospace Sciences Meeting and Exhibit (p. 176).
- Katz, J. and Plotkin, A. (2001) *Low-Speed Aerodynamics*, 2nd Ed., Cambridge University Press, 2001.
- Messinger, B. L. (1953) *Equilibrium Temperature of an Unheated Icing Surface as a Function of Air Speed*, Journal of the Aeronautical Sciences, 20, pp. 29-42.
- Myers, T. G., (2001) *Extension of the Messinger Model for aircraft icing*, AIAA J., Vol 39, p:211-218, 2001.
- Özgen, S., Canıbek, M. (2009) *Ice accretion simulation on multi-element airfoils using Extended Messinger Model*, Heat and Mass Transfer 45, p. 305-322, 2009.
- Özgen, S., Canıbek, M., Korkem, B. and Ortakaya, Y. (2007) *Ice shape prediction on airfoils using Extended Messinger method*, in 4th Ankara International Aerospace Conference, Ankara, Turkey, 2007.

Özgen, S., Tarhan, E., Canıbek, M. (2001) *3-D in-flight icing simulations and use of parallel computing in Lagrangian droplet trajectory calculations*, in 6th Ankara International Aerospace Conference, Ankara, Turkey, 2011.

Paraschiviou, I., Saeed, F. (2007) *Aircraft Icing*, John Wiley & Sons, New York, 2007.

Ruff, G. A., Duesterhaus, D. A. (1985) *Analysis and Verification of the Icing Scaling Equations Analysis and Verification*, UNITED STATES AIR FORCE, December 1985.

Wright, W. B., Gent, R. W. and Guffond, D. (1997) *DRA/NASA/ONERA collaboration on icing research, Part II-prediction of airfoil ice accretion*, NASA CR-202349, 1997.

APPENDIX

Cases given in [Wright, Gent and Guffond, 1997].

	Figure	Airfoil	Chord (m)	AOA (deg)	V (m/s)	Static Temp. (K)	Static Temp. (C)	Total Temp. (c)	Pressure (Pa)	LWC (g/m ³)	MVD (microns)	Exposure Time (s)
NASA	27	NACA0012	0.53	4	58.1	245.2	-27.8	-26	95610	1.3	20	480
	28		0.53	4	58.1	253.2	-19.8	-18	95610	1.3	20	480
	29		0.53	4	58.1	259.1	-13.9	-12	95610	1.3	20	480
	30		0.53	4	58.1	266.3	-6.7	-5	95610	1.3	20	480
	31		0.53	4	58.1	269.1	-3.9	-2	95610	1.3	20	480
	32		0.53	4	58.1	270.2	-2.8	-1	95610	1.3	20	480
	33		0.53	4	93.89	242.5	-30.5	-26	92060	1.05	20	372
	34		0.53	4	93.89	256.4	-16.6	-12	92060	1.05	20	372
	35		0.53	4	93.89	260.8	-12.2	-8	92060	1.05	20	372
	36		0.53	4	93.89	266.4	-6.6	-2	92060	1.05	20	372
DRA	37		0.53	0	130.5	260.7	-12.3	-3.8	90500	0.5	17.5	120
	38		0.53	8.5	130.5	260.7	-12.3	-3.8	90500	0.5	17.5	120
	39		0.53	8	131.5	269.1	-3.9	4.7	85000	0.6	20	180
ONERA	40	SA13112	0.6	10	81.3	263	-10	-6.7	79500	0.5	20	900
	41		0.6	0	162.5	263	-10	3.2	79500	0.5	20	450
	42		0.6	0	249.9	243	-30	1.2	79500	0.5	20	180